Cell Proliferation

Cell Prolif., 2015, **48**, 465–474 doi: 10.1111/cpr.12192

Independent effect of polymeric nanoparticle zeta potential/surface charge, on their cytotoxicity and affinity to cells

Xiao-Ru Shao*, Xue-Qin Wei*, Xu Song†, Li-Ying Hao*, Xiao-Xiao Cai*, Zhi-Rong Zhang†, Qiang Peng* and Yun-Feng Lin*

**State Key Laboratory of Oral Diseases, West China Hospital of Stomatology, Sichuan University, Chengdu 610041, China and †Key Laboratory of Drug Targeting and Drug Delivery Systems, Ministry of Education, West China School of Pharmacy, Sichuan University, Chengdu 610041, China*

Received 7 January 2015; revision accepted 1 March 2015

Abstract

Objectives: Up to now, little research has been focussed on discovering how zeta potential independently affects polymeric nanoparticle (NP) cytotoxicity.

Methods: Polymeric nanoparticles of gradient zeta potential ranging from −30 mv to +40 mv were fabricated using the same poly-3-hydroxybutyrate-co-3-hydroxyhexanoate (PHBHHx) biopolymer. Interaction forces between nanoparticles and cells were measured by atomic force microscopy (AFM). Cytotoxicity of the nanoparticles to cells was investigated by using MTT (3-(4,5-dimethyl-2-thiazolyl)-2,5-diphenyl-2-H-tetrazolium bromide) assay.

Results: Four kinds of nanoparticle with similar sizes and gradient zeta potentials, were fabricated. Those with positive surface charges were found to be more toxic than those with negative surface charges. Positively charged nanoparticles or nanoparticles with higher 'like' charges, offered higher interaction force with cells.

Conclusion: This work proposes a novel approach for investigating interaction between NPs and cells, and discloses the importance of controlling zeta potential in developing NPs-based formulations in the future.

Correspondence: Q. Peng and Y.F. Lin, State Key Laboratory of Oral Diseases, West China Hospital of Stomatology, Sichuan University, Chengdu 610041, China. Tel.: +86 28 85501484; Fax: +86 28 85501484; E-mail: lijm2002@163.com and Tel.: +86 28 85503487; Fax: +86 28 85503487; E-mail: yunfenglin@scu.edu.cn
Xiao-Ru Shao and Xue-Qin Wei contributed equally to this work.

Introduction

Nanoparticles (NPs) have been widely investigated for decades, this largely being due to their special properties, such as nanoscale size and large surface area. NPs have shown great potential for use in the fields of biomedical and life sciences (1–7). Several reports on NP applications in drug/gene delivery, *in vivo* imaging, as well as disease diagnosis and treatment have been well-documented (8–13). Despite these promising and encouraging study reports, comprehensive understanding of NPs is highly limited, especially concerning their interactions with cells, and also potential toxicity.

It has recently been found that NP performance can be substantially changed due to formation of protein coronas surrounding them (14–17). Our previous work has also shown that formation of albumin corona significantly changes basic NP physicochemical properties, their associated bio-responses, and also their toxicity (18). Formation and composition of protein coronas are largely dependent on NP size and their surface properties, including hydrophilicity/hydrophobicity, biocompatibility and zeta potential/surface charge (19,20). NP interactions with proteins are therefore determined by their size and surface properties.

NP particle size and surface chemistry also influence their interactions with, and toxicity to cells. Although the past decades have witnessed significant nanotechnology progress in various areas, potential nanotoxicity derived from extremely small nano-sized NPs, with large surface area to volume ratio, has been a critical research issue which has to be addressed before nano-products can be commercialized for large scale use (21). More attention particularly needs to be paid to nanotoxicity when NPs are designed for biomedical use, since nanoscale particles will be directly exposed to bodily fluids, cells and organs (22–24). Toxicity induced by

NPs can be varied between different types of NPs, according to their different properties. Understanding factors that affect NP nanotoxicity is thus important, to know how to efficiently predict and minimize it.

Factors impacting NP nanotoxicity are their basic physicochemical properties, such as particle size, shape, zeta potential, surface roughness, surface hydrophobicity, and biocompatibility (21). A plethora of articles has reported effects of particle size, shape, hydrophobicity, and biocompatibility on nanotoxicity (23,25,26), but there are very few which demonstrate effects of negative or positive surface charges on toxicity, from metal or carbon nanomaterials (27,28). Moreover, research is lacking on discovery of how zeta potential independently affects polymeric NP toxicity. NP surface charge, which can either be negative or positive (based on employed material properties and fabrication methods) (29–34), is one of the most critical, influencing functions of NPs.

In this work therefore, we have aimed to fabricate four polymeric NP systems, with different zeta potentials (including both negative and positive zeta potentials), investigating their effect on polymeric NP cytotoxicity, and disclosing its mechanisms by quantifying interaction force between NPs and cells.

Materials and methods

Materials

Poly-3-hydroxybutyrate-co-3-hydroxyhexanoate (PHBHHx) containing 14 mol% R-3-hydroxyhexanoate, with 175 000 Mw, was obtained from Lukang Group (Shandong, China). Poloxamer 188 (F68) was kindly donated by BASF (China) Co. Ltd. (Shanghai, China). Sodium deoxycholate (DOC-Na) and octadecylamine (OA) were supplied by Amresco (Solon, OH, USA). All other chemicals and reagents were of analytical grade.

Preparation of NPs with different zeta potentials

A biocompatible biopolyester PHBHHx was used as the main biomaterial for NP preparation. PHBHHx NPs with negative zeta potential were prepared according to previous reports, with some modifications (8,18,35). Briefly, 20 mg PHBHHx was dissolved in chloroform and the resultant organic solution was mixed with an aqueous solution containing 0.1% (m/v) F68, and different amounts of sodium deoxycholate, 1:20 volume ratio. The mixture was then immediately sonicated under different conditions and NPs were obtained after emulsion evaporation for 20 min at room temperature. When preparing positively charged NPs, 20 mg PHBHHx and certain amounts of octadecylamine were co-dissolved in chloroform and the resultant organic solution was mixed with 0.1% F68 solution at 1:20 volume ratios. Subsequent processes were the same as above and detailed fabrication parameters are listed in Table 1.

Physicochemical characterization of NPs

Particle size, size distribution and zeta potential of the various NPs were measured using dynamic light scattering and electrophoretic light scattering technologies using Zetasizer Nano ZS90 (Malvern Instruments Ltd., Worcestershire, UK). Particle size was presented by intensity distribution, and size distribution was evaluated by polydispersity index (PDI).

Morphology of NPs was characterized using scanning electron microscopy (SEM, INSPECT F, FEI, Netherland) and the freshly prepared NPs were diluted with distilled water 100–200-fold. One drop of diluted NP solution was placed on mica sheets, and after air-drying, samples were coated with gold before SEM characterization measurements.

Colloidal stability of NPs

A single aliquot of freshly prepared NPs (1 ml) was added to each centrifuge tube and incubated at 37 °C. Particle size of each NP was measured and compared at different time intervals (0, 6, 24, 48 and 72 h), to indicate their thermodynamic stability. In addition, 0.2-ml aliquot from upper layers of liquid was collected at the same fixed time intervals. Transmittance values from collected samples were recorded at 550 nm and compared, to indicate NP kinetic stability (36,37).

Cytotoxicity

Cytotoxicity of the various NPs was examined by MTT (3-(4,5-dimethyl-2-thiazolyl)-2,5-diphenyl-2-H-tetrazolium bromide) assay on mouse L929 fibroblasts.

Table 1. Detailed parameters for fabricating NPs of various zeta potentials

Samples no.	PHBHHx (mg)	OA (mg)	F68 (%, w/v)	DOC-Na (%, w/v)	Sonication time (s)
NPs-1	20	0	0.1	0.02	30
NPs-2	20	0	0.1	0.05	15
NPs-3	20	0.15	0.1	0	50
NPs-4	20	0.25	0.1	0	30

Briefly, cells were plated on 96-well culture plates at 2000 cells/well and cultured at 37 °C in 5% CO_2 for 24 h. Culture medium was then discarded and cells were then exposed to different NP concentrations dispersed in blank culture medium. Cultured cells in the blank culture medium served as controls. MTT assay medium was added to each well at predetermined time intervals (24, 48 or and 72 h), followed by further incubation for 4 h. It was then replaced with dimethyl sulphoxide and absorbance from the resulting solution detected at 490 nm. Cell viability was determined as percentage absorbance of treated cells to that of controls.

In addition to MTT assay, cells were stained with Calcein-AM fluorescent dye and propidium iodide (PI) with NP exposure to 50 μg/ml for 24 h, to differentiate between living and dead cells respectively. Briefly, L929 cells were plated on 48-well cell culture plates at 10 000 cells/well and cultured at 37 °C in 5% CO_2 for 24 h. Culture medium was then replaced by fresh medium containing 50 μg/ml NP and culturing was continued for 24 h. Culture medium containing NPs was subsequently discarded and cells were washed in PBS buffer (0.01 M, pH 7.4) containing 2 μM Calcein-AM; 4 μM PI was then added. Cells were then washed in fresh PBS followed by observation using fluorescence microscopy.

Interaction force between NPs and cells

Interaction between the various NPs and L929 cells was determined using atomic force microscopy (AFM, SPM9600; Shimadzu, Kyoto, Japan) contact model. Briefly, cells were cultured on clean, round glass coverslips placed in the 48-well plate; culturing conditions were the same as above. AFM cantilever tips were immersed into various NP solutions, followed by air-drying, so that the tips were coated with NPs. Culture medium was discarded after 24 h culture and cells-loaded coverslips were rapidly removed for AFM measurement, using the NP-coated cantilever under contact model. Interactions between NPs with randomized three cell positions were measured, and ten measured pieces of data from each position were recorded.

Statistical analysis

All data shown in this study are presented as mean ± SD (standard deviation). One-way analysis of variance was used to compare differences between groups, considered to be statistically significant when P values were <0.05.

Results

Preparation and physicochemical characterization of NPs

To exclude effects other than zeta potential from other factors, we prepared NP with desired zeta potentials by adjustment of surfactant type and amount, while maintaining all the other conditions to be identical (Table 1). Four kinds NP, as a result had similar size, over the narrow range of 220–245 nm (Fig. 1). In contrast, zeta potentials from these NPs were significantly different, increasing from −30 mv to +40 mv. In detail, mean zeta potentials of the obtained NPs were −21.2 mv for the NPs-1, −28.0 mv for the NPs-2, 20.0 mv for the NPs-3, and 44.9 mv for the NPs-4.

In addition to particle size and zeta potential value, their distributions were also an important parameter for evaluating quality of the NPs system. As shown in Fig. 2, size distribution of negatively charged NP-1 and NP-2 categories presented single, narrow peaks while positively charged NP-3 and NP-4 categories had double peaks. Size distribution is usually also presented as PDI, a numerical value in the range of 0–1, the lower the value the better the NPs (38). PDI values from obtained NPs were calculated as 0.136 for NP-1, 0.098 for NP-2, 0.194 for NP-3, and 0.188 for NP-4 (Fig. 2). The above results indicate that negatively charged NPs had better size distribution than positively charged ones as described in this work, although PDI values from all the NPs were quite acceptable (PDI < 0.3 means a good size distribution). Unlike size distribution, zeta potential distribution of all the kinds of NPs lay in a narrow range, indicating good zeta potential distribution for each type of NP.

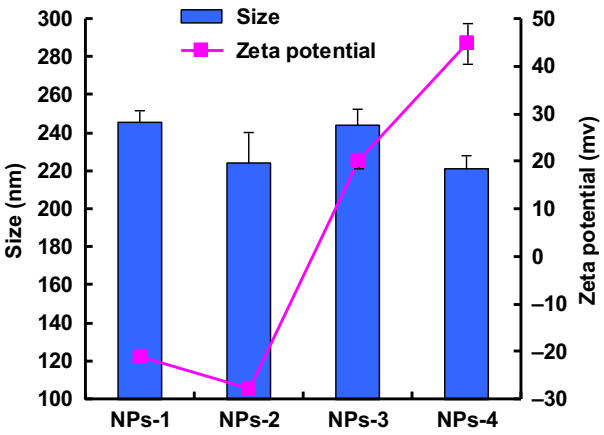

Figure 1. Size and zeta potential of four kinds of polymeric NP, prepared from the same biopolymer PHBHHx. Data presented as mean ± SD (n = 3).

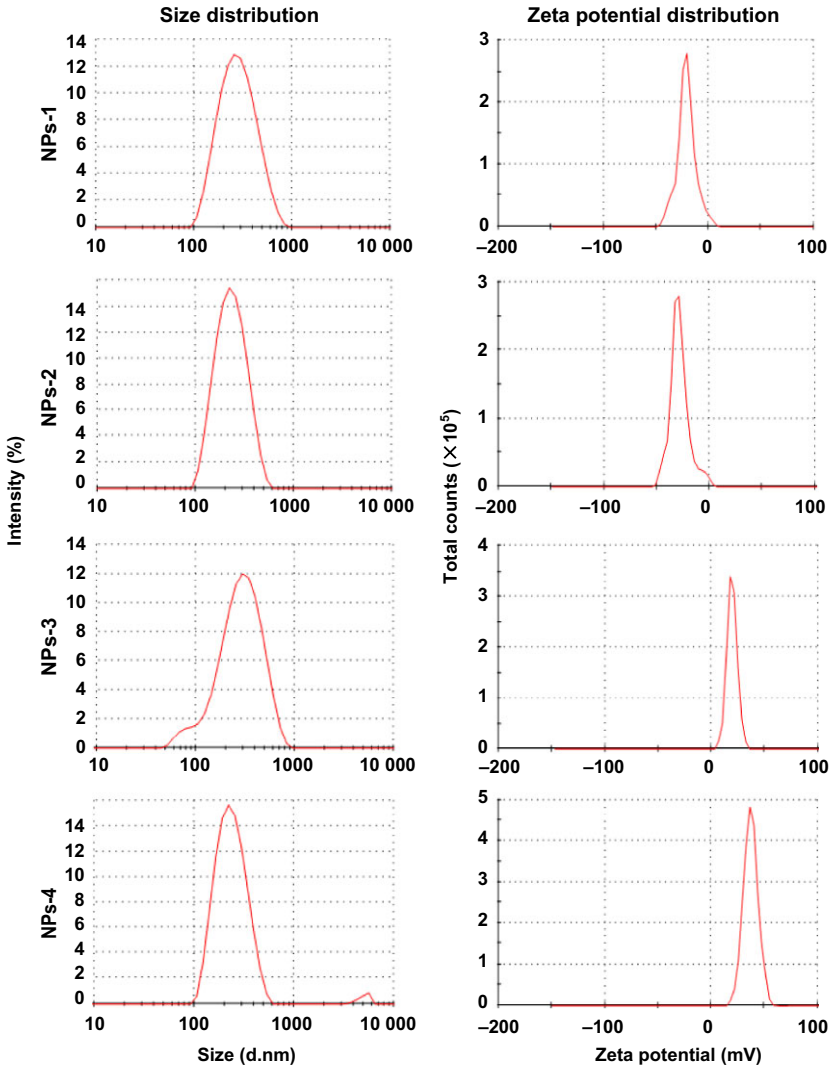

Figure 2. Typical size and zeta potential distribution graphs of the four kinds of NP.

Morphology was another critical indicator for quality evaluation of the NP system and was analyzed by using SEM. As shown in Fig. 3, the four kinds of NP were all spherical in shape, implying that zeta potential had no shape effect. We also saw that particle size of each type of NP was evenly-distributed, indicating their good size distribution, which was consistent with results derived from the dynamic light scattering measurement (Fig. 2).

Colloidal NP stability

Nanoparticles exist as a colloidal system and thus their colloidal stability has substantial impact for their storage and safety, and for application of NP-based formulations. In this work we investigated both thermodynamic and kinetic stabilities of the NPs, to monitor their particle size change and particle sedimentation rate, respectively. As shown in Fig. 4a, relative sizes of NP-1, NP-2 and NP-3 categories were comparable to their corresponding sizes at 0 h, which were in the 99–100% range and 97–100% range for NP-4 throughout the experiment. These results indicate that size of each type of NP had no significant change for at least 72 h. In other words, all four kinds of NP had high thermodynamic stability for at least 72 h at 37 °C.

Unlike high thermodynamic stabilities from all four NP systems, NP kinetic stabilities varied depending on their surface charges. NP suspensions are able to absorb incident light in a particle concentration-dependent manner; thus kinetic instability (that is, sedimentation) of NPs results in reduction in absorbance or increase in transmittance. As shown in Fig. 4b, transmittance from all four NP systems increased over the 72 h time period, but extents were different from each other. NP-2 with

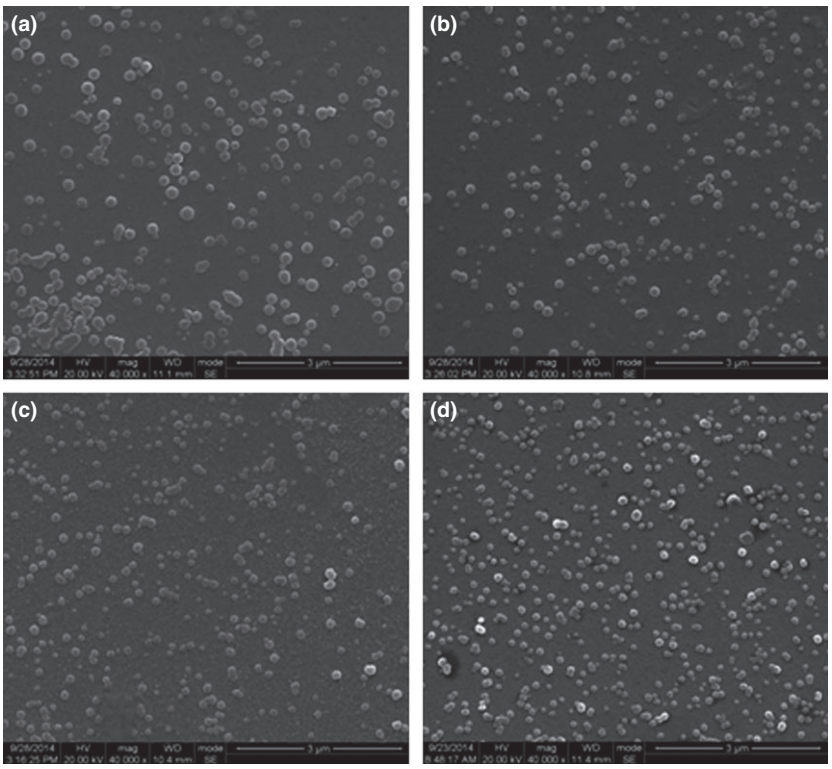

Figure 3. SEM images. (a) NP-1s, (b) NP-2s, (c) NP-3s and (d) NP-4s. Scale bar: 3 μm.

higher negative surface charge (−28 mv) had the smallest increases throughout the experiment. NP-1 with lower negative surface charge (−21 mv) and NP-4 with higher positive charge (45 mv) exhibited similar increases which were higher than NP-2 at each time point. NP-3 with lower positive charge (20 mv) also had significant increases over time. NP-3 relative transmittance was similar to that of NP-2 at 24 h (~120%) and increased to 190% at 48 h, which was similar to NP-1 and NP-4 categories. It then grew to 300% at 72 h. These results indicated that; (i) NP-2 had the highest kinetic stability, while NP-1 and NP-4 had medium stability, and NP-3 had the lowest kinetic stability; (ii) NPs with higher 'like' charges had higher kinetic stability; and finally (iii) NPs with negative surface charge had higher kinetic stability than those with equal positive charges.

Cytotoxicity of NPs

Nanotoxicity is one of the most critical issues that need to be addressed for nano-product development. Although it has been widely investigated, independent zeta potential effects on NP cytotoxicity have never previously been reported. We have demonstrated above that our four kinds of NP were prepared using the same PHBHHx biopolymer, possessing similar properties and gradient zeta potentials from −30~+40 mv, which were favourable for this study. MTT assay result, after exposure L929 cells to the NPs are shown in Fig. 5. It is clear that: (i) each type of NP presented a certain extent of cytotoxicity in a concentration-dependent manner, no matter how long the cells were exposed to them. In other words, higher particle concentration led to severe cytotoxicity. (ii) Cell survival rate decreased when NP exposure time was prolonged, for each type of NP, at different concentrations. (iii) Most importantly, NP cytotoxicity was in a zeta potential-dependent manner at different time points and particle concentration. In detail, negatively charged NPs (NP-1 and NP-2 categories) had lower cytotoxicity than positive ones (NP-3 and NP-4 categories). Moreover, NP-1 with lower negative surface charge than NP-2 led to higher levels of cells survival. NP-3 with lower positive surface charge than NP-4 similarly caused higher levels of cell survival, although NP-3 exposure concentration might have been higher due to their more rapid sedimentation rate (Fig. 4). NPs with larger similar charges were therefore more toxic to the cells, and the NPs, by category, exhibited the following order of cytotoxicity: NP-1 < NP-2 < NP-3 < NP-4.

Interaction force between NPs and cells

To confirm differential interaction between NPs and cells, we quantified their interaction force using the

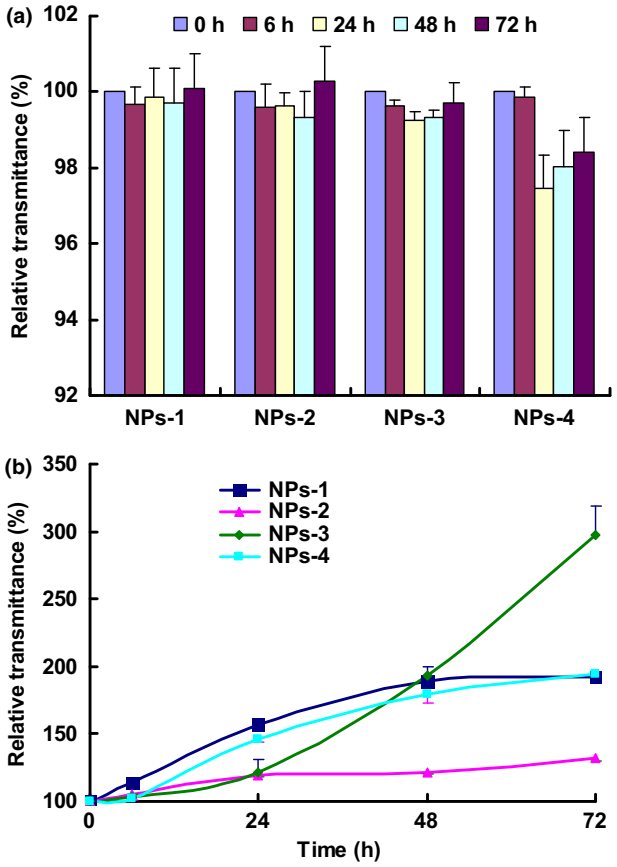

Figure 4. Colloidal stability of the four kinds of NP over a 72 h period at 37 °C. (a) Thermodynamic stability of NPs, measuring particle size change; (b) Kinetic stability of NPs measuring transmittance change of NP suspensions. Data presented as mean ± SD (n = 3).

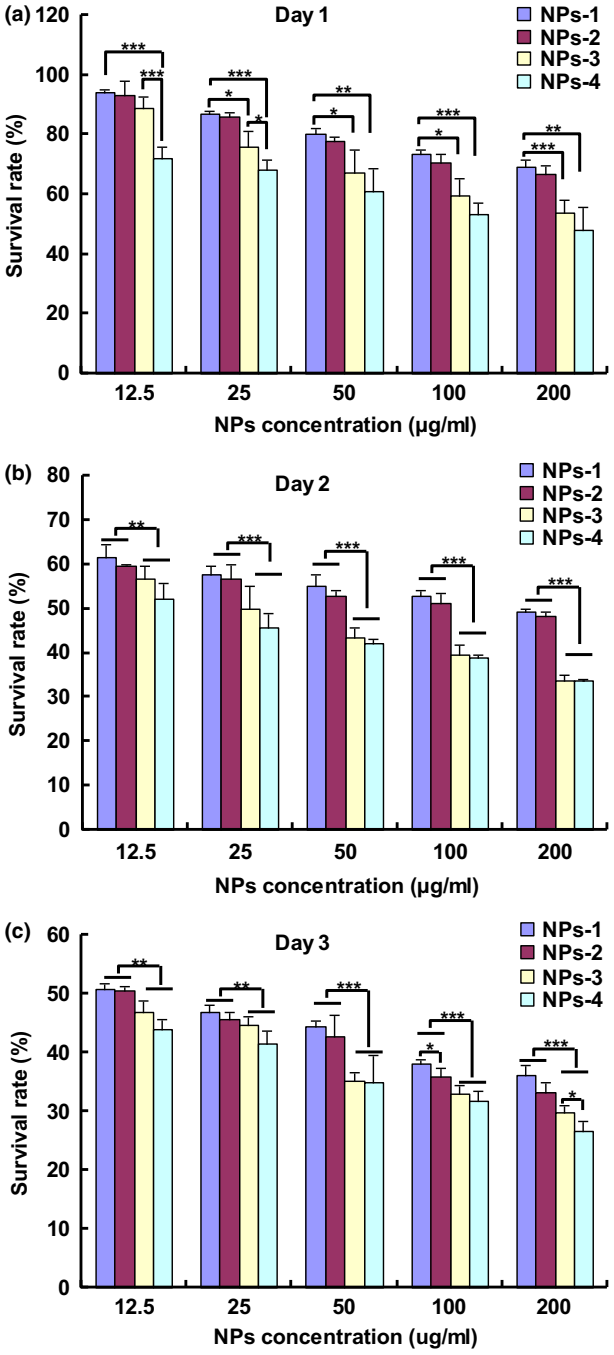

Figure 5. Cytotoxicity of the four kinds of NP with gradient zeta potentials (NP-1s: −21 mv; NP-2s: −28 mv; NP-3s: 20 mv and NP-4s: 44.9 mv) at five particle concentrations. (a) Incubation for 24 h, (b) 48 h and (c) 72 h. Data presented as mean ± SD (n = 4). Statistical significance: *P < 0.05, **P < 0.01, ***P < 0.001

AFM. As shown in Fig. 7a, force between cells and NP-1s was 2.7 nN, and slightly increased to 4.5 nN for NP-2s with cells, indicating that negatively charged NPs had a relatively weak interaction with the cells. In contrast, interaction force between cells and NP-3s became 8.8 nN (almost double that of NP-2s), and intensively increased to 20.2 nN for NP-4s with cells (Fig. 7a), indicating significantly stronger interaction between positively charged NPs with cells. As the four kinds of NP were fabricated using the same biopolymer and had similar sizes, the varied zeta potentials had to be the sole factor leading to their differential interaction forces. It is therefore likely that stronger interaction force resulted in higher cytotoxicity from positively charged NPs.

The interaction process can be observed from Fig. 7b; it occurred when NP-coated tips approached cells and then the tip was released. Extra force was needed to overcome interaction force, to completely release the tip and the force curve returned to being linear once the tip was thoroughly parted from the cells. To the best of our knowledge, this is the first study showing quantification of interaction force between NPs and cells. The results from this study thus provide solid

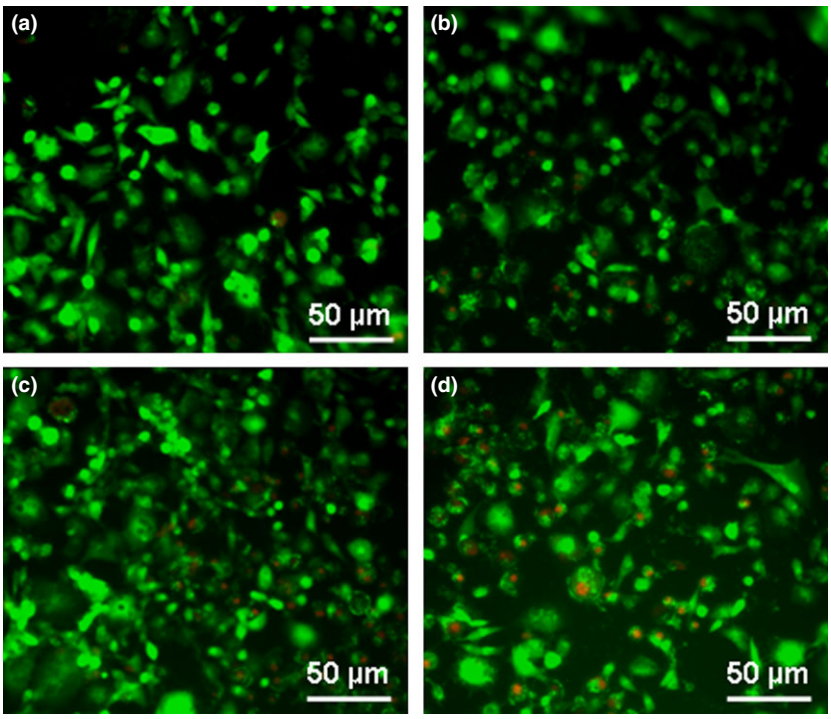

Figure 6. Fluorescence microscopy of L929 cells stained with Calcein-AM (green for living cells) and propidium iodide (PI, red for dead cells) for 24 h exposure to four kinds of NP at particle concentration of 50 μg/ml. (a) NP-1s: −21 mv; (b) NP-2s: −28 mv; (c) NP-3s: 20 mv and (d) NP-4s: 44.9 mv. Scale bar: 50 μm.

evidence for stronger reactivity of positively charged NPs, as probably the ultimate reason for their higher cytotoxicity.

Discussion

In this study, the biopolymer PHBHHx was used as carrier material to fabricate NPs. PHBHHx has been widely used in tissue engineering largely due to its biocompatibility, biodegradability and adjustable mechanical properties (39–41); PHBHHx potential in drug delivery has also been recently developed (8,42,43). Addition of ionic surfactants during fabrication of PHBHHx NPs was necessary due to strong PHBHHx hydrophobicity, to obtain well-dispersed NP suspensions. Added ionic surfactants were the exact sources of NP zeta potentials. In this work, the sodium deoxycholate anionic surfactant conferred negative zeta potential to NP-1 and NP-2 categories, and octadecylamine cationic surfactant conferred the positive charge to NP-3 and NP-4 categories. Amount of surfactant present can affect not only zeta potential but also particle size. There were therefore only few options when fabricating NPs, to obtain similar sizes.

Agglomeration and sedimentation are the two most common stability issues for NP systems (44). NPs have very high surface energy as a result of their extremely small particle size, and they tend to agglomerate to reduce energy spread, resulting in thermodynamic instability. Agglomeration has significant impact on NP safety, as agglomerated large particles carry high risk for capillary blockade after intravenous administration (45). Addition of non-ionic or ionic surfactant is the main approach for stabilizing nanosuspensions (46). Non-ionic surfactant such as F68 used in this work, forms a layer of protective coating surrounding the NPs and functions as a steric barrier to prevent particle agglomeration. In the case of ionic surfactant, such as sodium deoxycholate or octadecylamine used here, anionic or cationic moieties confer zeta potentials on NP. Electrostatic repulsive forces between particles play important roles in preventing agglomeration.

In common with all other particles, NPs also tend to sediment due to normal gravitational pull, resulting in kinetic instability. Factors, including particle size, particle density and zeta potential, medium density, and viscosity, can influence sedimentation. When other conditions are kept constant, larger size and/or smaller zeta potential can lead to faster sedimentation which might have been the main reason for lowest kinetic stability of NP-3s (Fig. 4b).

NPs are considered to be reactive due to their small size, large relative surface area, and high surface energy. Reactivity offers NPs great potential for interacting with biological components such as cells. It is assumed that NP interactions with cells have significant impact on mitochondrial and cell membrane viability, oxidative stress, and pro-inflammatory gene activation (22,47). In this work, we used fluorescent dye PI to stain nuclei

whose membranes had broken. PI is a reddish fluorescent stain for nuclei, that can only enter cells with disrupted membranes (thus having become permeable). Calcein-AM was used to stain living cells. Active enzymes in living cells release free calcein, which fluoresces green due to released calcein rather than Calcein-AM. Very little red signal was observed in this part of the study, indicating that NPs with negative zeta potential caused little damage to cell membranes, probably due to their weak interactions with the cells (Fig. 6a,b). In contrast, NPs with positive zeta potentials caused severe cell membrane damage as stronger red fluorescence was observed (Fig. 6c,d). A likely explanation for this finding is that positively charged NPs may have had stronger interaction with the cells (Fig. 7), with negatively charged membranes, due to presence of negative phospholipids and/or proteins (21). In the physiological environment, protein coronas surrounding NPs may reduce their interactions with cell membranes, and NPs can be engulfed into lysosomes (48–50). Interaction between NPs and lysosomal membranes may then damage the lysosomes and affect subsequent biological processes. In the case of negatively charged NPs, their interactions with biomembranes are relatively weak despite formation of coronas, as the membranes are also negatively charged. As a result, these NPs may only cause low cytotoxicity. In the case of positively charged NPs, coronas may be more stable and thus their interaction with plasma membranes may be reduced. However, coronas may become degraded in lysosomes and positive surfaces of NPs become exposed again, leading to strong interaction with lysosomal membranes and significant resulting cytotoxicity (51,52).

In conclusion, here we fabricated four kinds of NP with similar sizes and gradient zeta potentials, and also for the first time investigated independent effects of zeta potential on NP cytotoxicity. Additionally, interactions between NPs and cells were studied using an AFM. To

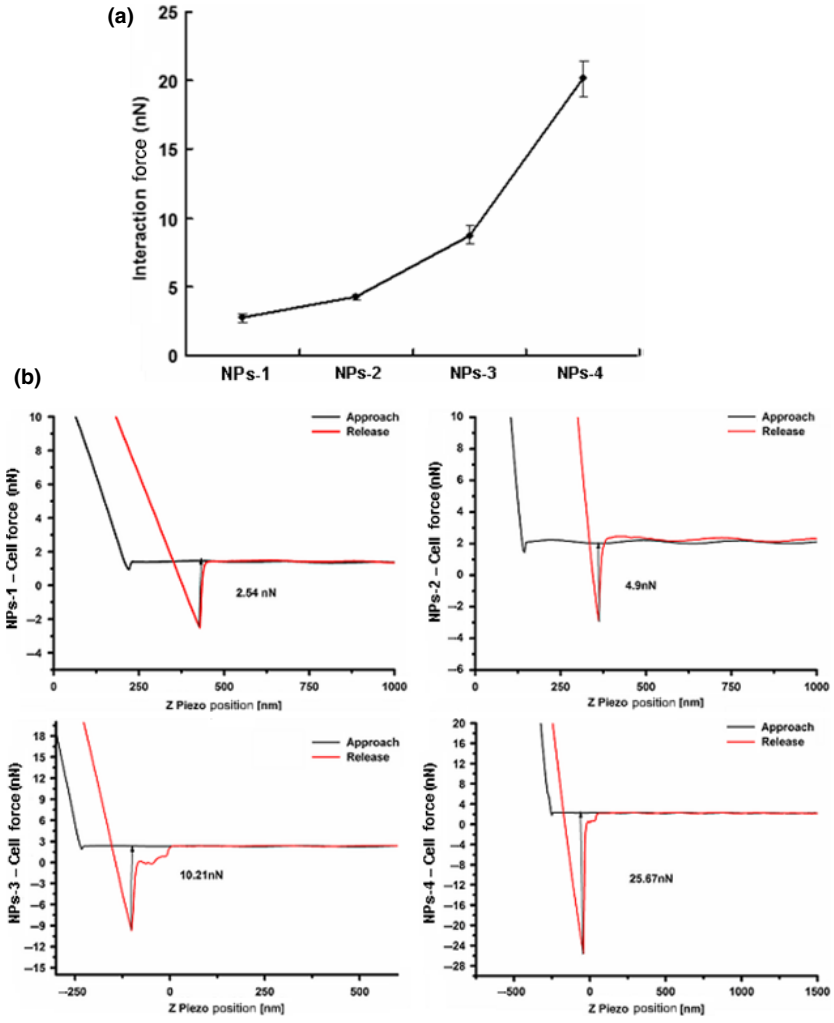

Figure 7. Quantification of interaction force between four kinds of NPs and L929 cells using AFM. (a) Interaction force of cells with NPs possessing various zeta potentials; (b) AFM force curves of each type of NPs with cells. NP-1s: −21 mv; NP-2s: −28 mv; NP-3s: 20 mv and NP-4s: 44.9 mv.

the best of our knowledge, this is the first investigation showing quantification of interactions between cells and NPs with gradient zeta potentials. Our findings showed that NPs with positive zeta potentials caused significantly higher cytotoxic effects than NPs with negative zeta potentials, and NPs with large similar charges were more toxic. The underlying mechanism was that NPs with positive surface charges or higher 'like' charges had stronger interactions with cells. This work proposes a novel approach for investigating interactions between NPs and cells and discloses the importance of controlling zeta potential in developing NP-based formulations in the future.

Acknowledgements

This work was funded by National Natural Science Foundation of China (31170929, 81201211, 81470721, and 81402860), Funding of Sichuan Province Youth Science and Technology Innovation Team (2014TD010), and Funding of State Key Laboratory of Oral Diseases (SKLOD201405).

Conflict of interests

The authors declare no competing financial interests.

References

1 Wang B, Galliford CV, Low PS (2014) Guiding principles in the design of ligand-targeted nanomedicines. *Nanomedicine (Lond)* **9**, 313–330.
2 Lalatsa A, Schatzlein AG, Uchegbu IF (2014) Strategies to deliver peptide drugs to the brain. *Mol. Pharm.* **11**, 1081–1093.
3 Jin L, Zeng X, Liu M, He N (2013) Chitosan/polylactic acid/tripolyphosphate nanocapsules for encapsulation of water-insoluble drugs: *in vitro* drug release and cytotoxicity. *Sci. Adv. Mat.* **5**, 2053–2057.
4 Zhang L, Wang Z, Lu Z, Shen H, Huang J, Zhao Q *et al.* (2013) PEGylated reduced graphene oxide as a superior ssRNA delivery system. *J. Mater. Chem. B* **1**, 749–755.
5 Kim TH, Choi H, Yu GS, Choi JS (2013) Synthesis of polyethylene glycol-oligo (glutamic acid) conjugated with polyethyleniminedexamethasone for gene delivery applications. *J. Nanosci. Nanotechnol.* **13**, 7325–7330.
6 Shah MAA, He N, Li Z, Ali Z, Zhang L (2014) Nanoparticles for DNA Vaccine Delivery. *J. Biomed. Nanotechnol.* **10**, 2332–2349.
7 Yang JH, Jung H, Kim SY, Yo CH, Choy JH (2013) Heterostructured layered aluminosilicate-itraconazole nanohybrid for drug delivery system. *J. Nanosci. Nanotechnol.* **13**, 7331–7336.
8 Peng Q, Zhang ZR, Gong T, Chen GQ, Sun X (2012) A rapid-acting, long-acting insulin formulation based on a phospholipid complex loaded PHBHHx nanoparticles. *Biomaterials* **33**, 1583–1588.
9 Gao LY, Liu XY, Chen CJ, Wang JC, Feng Q, Yu MZ *et al.* (2014) Core-shell type lipid/rPAA-Chol polymer hybrid nanoparticles for in vivo siRNA delivery. *Biomaterials* **35**, 2066–2078.
10 Jin L, Zeng X, Liu M, Deng Y, He N (2014) Current progress in gene delivery technology based on chemical methods and nano-carriers. *Theranostics* **4**, 240–255.
11 Wang T, Hu Y, Leach MK, Zhang L, Yang W, Jiang L *et al.* (2012) Erythropoietin-loaded oligochitosan nanoparticles for treatment of periventricular leukomalacia. *Int. J. Pharm.* **422**, 462–471.
12 Zhang L, Lu Z, Bai Y, Wang T, Wang Z, Chen J *et al.* (2013) PEGylated denatured bovine serum albumin modified water-soluble inorganic nanocrystals as multifunctional drug delivery platforms. *J. Mater. Chem. B* **1**, 1289–1295.
13 Shah MAA, Ali Z, Ahmad R, Qadri I, Fatima K, He N (2015) DNA mediated vaccines delivery through nanoparticles. *J. Nanosci. Nanotechnol.* **15**, 41–53.
14 Monopoli MP, Aberg C, Salvati A, Dawson KA (2012) Biomolecular coronas provide the biological identity of nanosized materials. *Nat. Nanotechnol.* **7**, 779–786.
15 Monopoli MP, Walczyk D, Campbell A, Elia G, Lynch I, Bombelli FB *et al.* (2011) Physical-chemical aspects of protein corona: relevance to in vitro and in vivo biological impacts of nanoparticles. *J. Am. Chem. Soc.* **133**, 2525–2534.
16 Lesniak A, Fenaroli F, Monopoli MP, Aberg C, Dawson KA, Salvati A (2012) Effects of the presence or absence of a protein corona on silica nanoparticle uptake and impact on cells. *ACS Nano* **6**, 5845–5857.
17 Salvati A, Pitek AS, Monopoli MP, Prapainop K, Bombelli FB, Hristov DR *et al.* (2013) Transferrin-functionalized nanoparticles lose their targeting capabilities when a biomolecule corona adsorbs on the surface. *Nat. Nanotechnol.* **8**, 137–143.
18 Peng Q, Zhang S, Yang Q, Zhang T, Wei XQ, Jiang L *et al.* (2013) Preformed albumin corona, a protective coating for nanoparticles based drug delivery system. *Biomaterials* **34**, 8521–8530.
19 Lundqvist M, Stigler J, Elia G, Lynch I, Cedervall T, Dawson KA (2008) Nanoparticle size and surface properties determine the protein corona with possible implications for biological impacts. *Proc. Natl Acad. Sci. USA* **105**, 14265–14270.
20 Zhang XQ, Xu X, Bertrand N, Pridgen E, Swami A, Farokhzad OC (2012) Interactions of nanomaterials and biological systems: implications to personalized nanomedicine. *Adv. Drug Deliv. Rev.* **64**, 1363–1384.
21 Sharifi S, Behzadi S, Laurent S, Forrest ML, Stroeve P, Mahmoudi M (2012) Toxicity of nanomaterials. *Chem. Soc. Rev.* **41**, 2323–2343.
22 Yildirimer L, Thanh NT, Loizidou M, Seifalian AM (2011) Toxicology and clinical potential of nanoparticles. *Nano Today* **6**, 585–607.
23 Lewinski N, Colvin V, Drezek R (2008) Cytotoxicity of nanoparticles. *Small* **4**, 26–49.
24 Zhang L, Lu Z, Li X, Deng Y, Zhang F, Ma C *et al.* (2012) Methoxy poly(ethylene glycol) conjugated denatured bovine serum albumin micelles for effective delivery of camptothecin. *Polym. Chem.* **3**, 1958–1961.
25 Soenen SJ, Manshian B, Doak SH, De Smedt SC, Braeckmans K (2013) Fluorescent non-porous silica nanoparticles for long-term cell monitoring: cytotoxicity and particle functionality. *Acta Biomater.* **9**, 9183–9193.
26 Wang T, Jiang X (2015) Breaking of phosphodiester bond: a key factor induced hemolysis. *ACS Appl. Mat. Interfaces* **7**, 129–136.
27 Goodman CM, McCusker CD, Yilmaz T, Rotello VM (2004) Toxicity of gold nanoparticles functionalized with cationic and anionic side chains. *Bioconjug. Chem.* **15**, 897–900.
28 Saxena RK, Williams W, McGee JK, Daniels MJ, Boykin E, Ian Gilmour M (2007) Enhanced in vitro and in vivo toxicity of poly-

dispersed acid-functionalized single-wall carbon nanotubes. *Nanotoxicology* **1**, 291–300.
29 Chen CJ, Wang JC, Zhao EY, Gao LY, Feng Q, Liu XY *et al.* (2013) Self-assembly cationic nanoparticles based on cholesterol-grafted bioreducible poly(amidoamine) for siRNA delivery. *Biomaterials* **34**, 5303–5316.
30 Peng Q, Wei XQ, Shao XR, Zhang T, Zhang S, Fu N *et al.* (2014) Nanocomplex based on biocompatible phospholipids and albumin for long-circulation applications. *ACS Appl. Mat. Interfaces* **6**, 13730–13737.
31 He B, Lin P, Jia Z, Du W, Qu W, Yuan L *et al.* (2013) The transport mechanisms of polymer nanoparticles in Caco-2 epithelial cells. *Biomaterials* **34**, 6082–6098.
32 Kulkarni SA, Feng SS (2013) Effects of particle size and surface modification on cellular uptake and biodistribution of polymeric nanoparticles for drug delivery. *Pharm. Res.* **30**, 2512–2522.
33 Moller P, Lykkesfeldt J (2014) Positive charge, negative effect: the impact of cationic nanoparticles in the brain. *Nanomedicine (Lond)* **9**, 1441–1443.
34 Zhao Y, Yu B, Hu H, Hu Y, Zhao NN, Xu FJ (2014) New low molecular weight polycation-based nanoparticles for effective codelivery of pDNA and drug. *ACS Appl. Mat. Interfaces* **6**, 17911–17919.
35 Peng Q, Wei XQ, Yang Q, Zhang S, Zhang T, Shao XR *et al.* (2015) Enhanced biostability of nanoparticle-based drug delivery systems by albumin corona. *Nanomedicine (Lond)* **10**, 205–214.
36 Moorkoth D, Nampoothiri KM (2014) Synthesis, colloidal properties and cytotoxicity of biopolymer nanoparticles. *Appl. Biochem. Biotechnol.* **174**, 2181–2194.
37 Kan KH, Li J, Wijesekera K, Cranston ED (2013) Polymer-grafted cellulose nanocrystals as pH-responsive reversible flocculants. *Biomacromolecules* **14**, 3130–3139.
38 Peng Q, Zhang ZR, Sun X, Zuo J, Zhao D, Gong T (2010) Mechanisms of phospholipid complex loaded nanoparticles enhancing the oral bioavailability. *Mol. Pharm.* **7**, 565–575.
39 Lomas AJ, Webb WR, Han J, Chen GQ, Sun X, Zhang Z *et al.* (2013) Poly (3-hydroxybutyrate-co-3-hydroxyhexanoate)/collagen hybrid scaffolds for tissue engineering applications. *Tissue Eng Part C. Methods* **19**, 577–585.
40 Wu Q, Wang Y, Chen GQ (2009) Medical application of microbial biopolyesters polyhydroxyalkanoates. *Artif. Cells Blood Substit. Immobil. Biotechnol.* **37**, 1–12.
41 Webb WR, Dale TP, Lomas AJ, Zeng G, Wimpenny I, El Haj AJ *et al.* (2013) The application of poly(3-hydroxybutyrate-co-3-hydroxyhexanoate) scaffolds for tendon repair in the rat model. *Biomaterials* **34**, 6683–6694.
42 Peng Q, Sun X, Gong T, Wu CY, Zhang T, Tan J *et al.* (2013) Injectable and biodegradable thermosensitive hydrogels loaded with PHBHHx nanoparticles for the sustained and controlled release of insulin. *Acta Biomater.* **9**, 5063–5069.
43 Peng Q, Yang YJ, Zhang T, Wu CY, Yang Q, Sun X *et al.* (2013) The implantable and biodegradable PHBHHx 3D scaffolds loaded with protein-phospholipid complex for sustained delivery of proteins. *Pharm. Res.* **30**, 1077–1085.
44 Wu L, Zhang J, Watanabe W (2011) Physical and chemical stability of drug nanoparticles. *Adv. Drug Deliv. Rev.* **63**, 456–469.
45 Patravale VB, Date AA, Kulkarni RM (2004) Nanosuspensions: a promising drug delivery strategy. *J. Pharm. Pharmacol.* **56**, 827–840.
46 Rabinow BE (2004) Nanosuspensions in drug delivery. *Nat. Rev. Drug Discov.* **3**, 785–796.
47 Carlson C, Hussain SM, Schrand AM, Braydich-Stolle LK, Hess KL, Jones RL *et al.* (2008) Unique cellular interaction of silver nanoparticles: size-dependent generation of reactive oxygen species. *J. Phys. Chem. B.* **112**, 13608–13619.
48 Wang F, Yu L, Monopoli MP, Sandin P, Mahon E, Salvati A *et al.* (2013) The biomolecular corona is retained during nanoparticle uptake and protects the cells from the damage induced by cationic nanoparticles until degraded in the lysosomes. *Nanomedicine* **9**, 1159–1168.
49 Anguissola S, Garry D, Salvati A, O'Brien PJ, Dawson KA (2014) High content analysis provides mechanistic insights on the pathways of toxicity induced by amine-modified polystyrene nanoparticles. *PLoS ONE* **9**, e108025.
50 Kim JA, Salvati A, Aberg C, Dawson KA (2014) Suppression of nanoparticle cytotoxicity approaching in vivo serum concentrations: limitations of in vitro testing for nanosafety. *Nanoscale* **6**, 14180–14184.
51 Wang F, Bexiga MG, Anguissola S, Boya P, Simpson JC, Salvati A *et al.* (2013) Time resolved study of cell death mechanisms induced by amine-modified polystyrene nanoparticles. *Nanoscale* **5**, 10868–10876.
52 Kim JA, Aberg C, de Carcer G, Malumbres M, Salvati A, Dawson KA (2013) Low dose of amino-modified nanoparticles induces cell cycle arrest. *ACS Nano* **7**, 7483–7494.

